

TOWARDS ADAPTING DEEP VISUOMOTOR REPRESENTATIONS FROM SIMULATED TO REAL ENVIRONMENTS

Eric Tzeng¹, Coline Devin¹, Judy Hoffman¹, Chelsea Finn¹, Xingchao Peng²,
Sergey Levine¹, Kate Saenko², Trevor Darrell¹

¹ University of California, Berkeley

² University of Massachusetts Lowell

ABSTRACT

We address the problem of adapting robotic perception from simulated to real-world environments. For many robotic control tasks, real training imagery is expensive to obtain, but a large amount of synthetic data is easy to generate through simulation. We propose a method that adapts representations using a small number of paired synthetic and real views of the same object/scene. Prior approaches to deep domain adaptation fail to exploit such paired instance constraints. Our proposed model generalizes prior approaches and combines a standard in-domain loss, a cross-domain adaptation loss, and a contrastive loss explicitly designed to align pairs of images in feature space. We evaluate our approach on robotic and object pose estimation and show that, by exploiting the presence of synthetic-real image pairs, our model is able to compensate for domain shift more effectively than standard adaptation techniques. Our results serve as an initial step toward pretraining deep visuomotor policies entirely in simulation, significantly reducing physical demands when learning complex policies.

1 INTRODUCTION

Deep reinforcement learning methods have shown remarkable performance and generality on tasks ranging from locomotion to playing Atari games (Mnih et al., 2013; Schulman et al., 2015; Lillicrap et al., 2015). Such models can be learned end-to-end, mapping observed pixels directly to actions. A key question has been whether such methods can be extended to work in the real world, where brute-force exploration of a policy parameter space with physical agents is infeasible.

Recent efforts have shown promising results on real-world manipulation through end-to-end learning using architectures designed to minimize network size, as well as sophisticated policy search methods to structure training (Levine et al., 2015; Finn et al., 2015). Such structured training can greatly reduce the number of physical trials. However, effective generalization to varied environments and objects is difficult with such limited datasets. Substantially longer interactions produce better generalization, but at a cost in time and effort that makes it impractical to learn large motion skill repertoires (Pinto & Gupta, 2015). In this paper we propose a complementary paradigm, which has the potential to remove such restrictions by transferring learned visual representations from synthetic simulated environments to the real world.

In both vision and robotics, it has long been a desirable goal to use synthetic rendered images to train models that are effective in the real world. Classically, hand-engineered features were designed to be invariant to the domain shift between synthetic and real worlds, e.g., efforts dating from the earliest model alignment methods in computer vision using edge detection-based representations. It is especially notable that one of the earliest visuomotor neural network learning methods, ALVINN (Pomerleau, 1989), exploited simulated training data of observed road shapes when training a multi-layer perceptron for an autonomous driving task. Many approaches to pose estimation in the recent decade were trained using rendered scenes from POSER and other human form rendering systems (Shakhnarovich et al., 2003; Urtasun & Darrell, 2008; Taylor et al., 2010); reliance on conventional feature representations limited their performance, however, and state-of-the-art pose estimation methods generally train exclusively on real imagery (Toshev & Szegedy, 2013; Tompson et al., 2014).

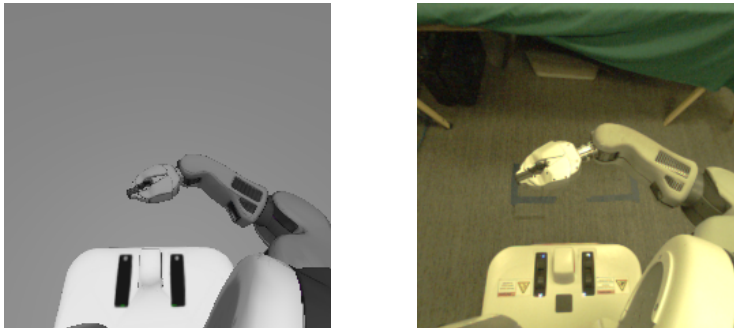


Figure 1: A pair of corresponding synthetic (left) and real-world (right) images. Simply training a model on synthetic images and testing on real-world images yields poor performance due to differences in fidelity and inaccurate renderings. In this particular example, not only is the rendering relatively low fidelity, but the gripper design on the synthetic model differs slightly from the gripper on the real robot. Despite these differences, by training on pairs like these, our method is able to learn from generated synthetic examples to perform pose estimation on real-world images.

Deep visual representations have been successfully trained from synthetic imagery (Su et al., 2015; Peng et al., 2015) and generally have a greater degree of domain invariance than conventional methods; nonetheless, as has been previously reported (Zhang et al., 2015) and our experiments below confirm for visuomotor CNNs, even state of the art deep models are still typically suboptimal when trained on synthetic data and tested on real data. Domain adaptation methods have been proposed in the literature to specifically optimize deep representations to be invariant to source-target domain bias in visual recognition tasks. We propose a similar paradigm for training deep convolutional visuomotor models, including those that incorporate deep spatial feature points (Levine et al., 2015).

Existing deep domain adaptation methods have focused on the category-level domain invariance task, and employed optimization which generally reduced the discrepancy or confusion between domains; this is valuable, but misses a significant opportunity in the setting of synthetic to real image adaptation. It is often feasible to align a small number of real images to a simulated environment, which provides very strong training constraints for a deep domain adaptation architecture. While such constraints have been explored in earlier adaptation schemes (Saenko et al., 2010), to our knowledge they have not been combined with contemporary deep discrepancy or deep confusion models. We propose a novel generalized framework, with losses for both pairwise and distribution alignment, and illustrate performance on variants of standard computer vision pose prediction tasks with modified PASCAL imagery.

As a first step towards our ultimate goal of demonstrating transfer of training of a full simulated visuomotor model to real environments, we also report experiments with our framework on the pose pretraining stage of the visuomotor model of Levine et al. (2015), using a real and simulated PR2 robot arm, as shown in Figure 1. Our results confirm (1) there is a significant domain shift between synthetic and real settings in visuomotor task learning, (2) that domain adaptation methods specialized to the deep spatial feature point architecture can learn to be relatively invariant to such shifts and improve performance, and (3) that inclusion of pairwise constraints provides a performance boost relative to previous deep domain adaptation approaches based solely on discrepancy minimization or domain confusion maximization. As increasingly sophisticated simulation environments become integrated into our system, we expect our model to support simulated pretraining of nearly the entire deep visuomotor pipeline, significantly reducing physical demands when training complex new tasks.

2 RELATED WORK

We present an algorithm which learns to adapt representation models trained using synthetically generated visual data to representations and models which can be effectively used to recognize in real world visual data.

Domain adaptation. We cast the shift from synthetic to real images as a domain adaptation problem. Classical visual domain adaptation methods tackled the problem where a fixed representation

extraction algorithm was used for both visual domains and adaptation took the form of learning a transformation between the two spaces (Saenko et al., 2010; Gopalan et al., 2011; Gong et al., 2012) or regularizing the target domain model based on the source domain (Yang et al., 2007; Aytar & Zisserman, 2011). Further models improved upon this by proposing adaptation which both transformed the representation spaces and regularized the target model using the source Duan et al. (2012); Hoffman et al. (2013). Since the resurgence in the popularity of convolutional networks for visual representation learning, adaptation approaches have been proposed to optimize the full target representation and model to better align with the source, for example by minimizing the maximum mean discrepancy (Tzeng et al., 2014; Long et al., 2015) or by minimizing the a-distance (specific form of discrepancy distance (Mansour et al., 2009)) between the two distributions (Ganin & Lempitsky, 2015; Tzeng et al., 2015).

Recently, method have been proposed to use 3D object models to render synthetic training examples for training visual models with limited human annotations needed (Sun & Saenko, 2014). It was shown that there is a specific domain shift problem that arises when applying a synthetically trained visual model to the real world data. This paradigm of synthetic to real was further used to study deep representations and what they learn by Peng et al. (2014).

Contrastive Loss for adaptation. It has been shown that a contrastive loss between the source and target points is an effective technique for transferring information. A contrastive metric learning loss was used for training a transformation from source to target domain for visual domain adaptation in Kulis et al. (2011) and Saenko et al. (2010). In those methods the learned adaptation was a kernelized transformation over a fixed representation. Earlier work introduced Siamese networks (Bromley et al., 1994; Chopra et al., 2005) for which a shared representation is directly optimized using the contrastive loss for signature and face verification and later for dimensionality reduction (Hadsell et al., 2006) and person hand and head pose alignment (Taylor et al., 2010). Taylor et al. (2010) further explored combining synthetic data along with real data to improve representation invariance and overall performance, however this method used the synthetic data to regularize the learning of the real model and found that performance suffered once the amount of simulated data overwhelmed the amount of real world data. In contrast, our approach uses synthetic data to learn a complete model and uses a very limited number of real examples for refining and adapting that model.

Visuomotor policy learning. The standard approach to processing visual input for robotic control is to use a discrete state estimation system to distill the visual signal into a low-dimensional state (e.g., the positions of objects in the world). This state is then used as a noisy input into the control policy (Pastor et al., 2009). Recently, there has been considerable interest in learning visuomotor policies directly from visual imagery using deep networks (Riedmiller et al., 2012; Levine et al., 2015; Watter et al., 2015; Lillicrap et al., 2015). This tight coupling between perception and control simplifies both the vision and control aspects of the problem, but suffers from the major limitation that each new task requires collection, annotation, and training on real world visual data in order to successfully learn a policy. To overcome this issue, we explore how simulated imagery can be adapted for robotic tasks in the real world. Directly applying models learned in simulation to the real world typically does not succeed (Zhang et al., 2015), due to systematic discrepancies between real and simulated data. We demonstrate that our domain adaptation method can successfully perform state estimation for a real robotic task using minimal real world data, suggesting that adaption from simulation to the real world can be effective for robotic learning.

3 TOWARDS TRAINING VISUOMOTOR POLICIES WITH VISUAL SIMULATION

We propose a visuomotor representation that pretrains on easily available simulated image inputs and adapts to real image inputs using a few supervised examples. Our representation is a crucial step towards simulation training of policies that receive pixels and output control parameters.

We build upon the end-to-end architecture presented by Levine et al. (2015) for training deep visuomotor policies that can learn to accomplish tasks such as screwing a cap onto a bottle or placing a coat hanger on a rack. The method first pretrains a convolutional neural network on a pose estimation task, then finetunes this network with guided policy search to map from input image to action. Guided policy search is initialized with trajectories from a fully observed state (where the locations of both the manipulated and target object are known), but once learned, the policy only requires visual input at test time.

We propose that this entire network could be trained in simulation and transferred to the real world using our adaptive visual network. This means that we can simulate the robot and its dynamics using a simulator (e.g., Gazebo), and can also simulate visual observations of manipulated objects through open sourced 3D models. Since the rendering and dynamics are imperfect, we propose the use of domain adaptation to bridge the gap.

Training in simulation not only significantly reduces training time, but also increases the variations seen during training. For example, although training a real PR2 with a thousand different objects would be infeasible to do by hand, we can programmatically generate thousands of different object models from CAD data and input them into the simulation.

In this paper we focus on solving the first critical step of pretraining the deep spatial feature point architecture using synthetic examples and then transferring the representation for use with real imagery. Success at this task supports the feasibility of visual transfer from rendered robotic environments to the real world in realistic scenarios.

4 GENERALIZED DOMAIN ALIGNMENT

Our method generalizes the approaches reviewed above and combines three core elements: a pose estimation loss, a domain confusion loss to align the synthetic and real domains in feature space, and a contrastive loss to align specific pairs in feature space. Together, these three losses ensure that we learn a representation that is conducive to the pose estimation task while remaining robust to the synthetic-real domain shift. Our model is novel in that it is the first deep adaptive model to explicitly exploit pairs of images to better mitigate domain shift and learn domain invariant representations.

The first loss function our method employs is a standard Euclidean loss on pose predictions. Given input images x and ground truth poses ϕ , we look to learn a representation θ_{repr} and a pose regressor θ_ϕ that minimizes the following pose estimation loss:

$$\mathcal{L}_\phi(x, \phi; \theta_\phi, \theta_{\text{repr}}) = \frac{1}{2K} \sum_i \|\theta_\phi^T f(x^{(i)}; \theta_{\text{repr}}) - \phi^{(i)}\|_2^2. \quad (1)$$

However, because images produced in simulation are generally of much lower fidelity than real-world images, we expect a pose estimator trained primarily on synthetic data to perform poorly when evaluated on real data. Thus, we would like to additionally ensure that the representation we learn, θ_{repr} , is resilient to the domain shift between synthetic and real images. To this end, we adopt the domain confusion loss introduced by Tzeng et al. (2015). This loss learns a domain classifier θ_D that attempts to correctly classify each image into the domain it originates from. It then attempts to learn a representation θ_{repr} such that the domain classifier cannot distinguish the two domains in feature space. This loss corresponds to the cross entropy loss between the predicted domain label of each image x and a uniform distribution over the D domains:

$$\mathcal{L}_{\text{conf}}(x_S, x_T, \theta_D; \theta_{\text{repr}}) = - \sum_{x \in (x_S \cup x_T)} \sum_d \frac{1}{D} \log q_d(x, \theta_D, \theta_{\text{repr}}). \quad (2)$$

Here, q corresponds to the domain classifier activations:

$$q(x, \theta_D; \theta_{\text{repr}}) = \text{softmax}(\theta_D^T f(x; \theta_{\text{repr}})) \quad (3)$$

Thus far we have modeled the synthetic-real shift as a standard visual domain adaptation problem, where the synthetic domain serves as our source, and the real-world domain serves as our target. However, unlike standard adaptation settings, the synthetic-real shift is unique in that it is possible to render a synthetic version of each real image. In doing so, we provide explicit examples of images that our representation should consider identical, thereby separating the irrelevant, domain-specific differences from the details relevant to performing pose estimation.

To incorporate these pairwise constraints between corresponding images, we employ the contrastive loss function introduced by Hadsell et al. (2006). This loss function seeks to draw paired images closer together in feature space while ensuring that unpaired images remain separated by at least some margin m . More formally, given a set P of pairs (i, j) such that $x_S^{(i)}$ and $x_T^{(j)}$ are paired, we

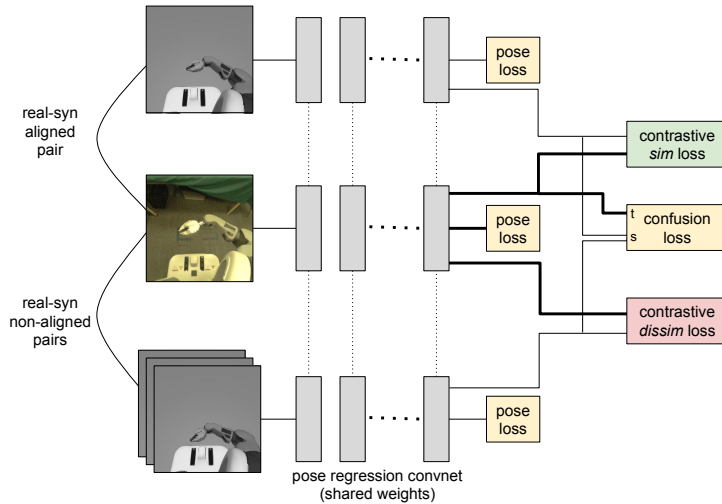


Figure 2: Generalized Domain Alignment architecture.

write our contrastive loss as

$$\mathcal{L}_{\text{contrast}}(x_S, x_T, P, \theta_{\text{repr}}) = \sum_{(i,j) \in P} \left[\frac{1}{2} D(x_S^{(i)}, x_T^{(j)}; \theta_{\text{repr}})^2 + \frac{1}{2(|x_S| - 1)} \sum_{k \neq i} \max\{0, m - D(x_S^{(k)}, x_T^{(j)}; \theta_{\text{repr}})\}^2 \right] \quad (4)$$

where we define our distance function D as the Euclidean distance in the feature space corresponding to θ_{repr} :

$$D(x_S^{(i)}, x_T^{(j)}; \theta_{\text{repr}}) = \left\| f(x_S^{(i)}; \theta_{\text{repr}}) - f(x_T^{(j)}; \theta_{\text{repr}}) \right\|_2. \quad (5)$$

Our particular formulation of the contrastive loss is modified slightly to explicitly weight matching and imposter pairs equally. In practice, this weighting is achieved by optimizing over minibatches that sample an equal number of each kind of pair.

Our full model thus minimizes the joint loss function

$$\begin{aligned} \mathcal{L}(x_S, \phi_S, x_T, \phi_T, P, \theta_D; \theta_\phi, \theta_{\text{repr}}) &= \mathcal{L}_\phi(x_S, \phi_S; \theta_\phi, \theta_{\text{repr}}) + \mathcal{L}_\phi(x_T, \phi_T; \theta_\phi, \theta_{\text{repr}}) \\ &+ \lambda \mathcal{L}_{\text{conf}}(x_S, x_T, \theta_D; \theta_{\text{repr}}) \\ &+ \nu \mathcal{L}_{\text{contrast}}(x_S, x_T, P; \theta_{\text{repr}}) \end{aligned} \quad (6)$$

where the hyperparameters λ and ν trade off how strongly we enforce domain confusion and pairwise constraints.

We depict the architecture setup for a given sampled real image in Figure 2. For the target real image, we have access to an aligned synthetic image (*top image* Fig 2) as well as other synthetic images which are not aligned with the real image (non-aligned). The standard pose loss is applied to all images the network sees, regardless if they arise from synthetic or real processes. Each synthetic-real pair is input to the contrastive loss which seeks to make the points similar if they are aligned examples and dis-similar if they are non-aligned examples. Finally, all synthetic (source) examples as well as all real (target) examples are additionally optimized by the confusion loss, which seeks to make the representation agnostic to whether synthetic or real imagery was input to the network.

The combination of losses presented here is architecture-agnostic, thereby making our method applicable to many different pose estimation models. For this paper, we apply our method to a version of the standard Krizhevsky architecture (Krizhevsky et al., 2012) modified to perform azimuth estimation on airplane imagery, as well as the deep spatial feature point network used by Levine et al. (2015) to learn visuomotor policies for manipulation tasks.



Figure 3: An example synthetic rendering of an airplane (left) using the pose from an actual PASCAL airplane example (right).

Method	Accuracy at θ				Average
	$\theta = \frac{\pi}{4}$	$\theta = \frac{\pi}{8}$	$\theta = \frac{\pi}{16}$	$\theta = \frac{\pi}{24}$	
Synthetic only	39.94%	22.19%	11.83%	7.69%	20.41%
Real only	44.08%	22.49%	11.83%	9.76%	22.04%
Synthetic and real	46.15%	25.15%	12.13%	9.17%	23.15%
Domain confusion (Tzeng et al., 2015)	48.22%	27.81%	16.27%	10.36%	25.67%
Contrastive loss	47.63%	28.40%	16.57%	10.65%	25.81%
Generalized domain alignment	50.00%	30.47%	15.09%	8.58%	26.26%
Oracle	56.21%	34.91%	18.05%	13.31%	30.62%

Table 1: Evaluation results on PASCAL airplane pose estimation when limiting ourselves to only 17 real examples. Each real example is paired with a corresponding synthetic image in the same pose, and an additional 321 unpaired synthetic images are also provided as training data. Each column reports the percentage of examples correctly estimated with error less than some angle threshold θ . We see that the methods that can make use of paired synthetic and real images outperform other standard adaptation methods. We also see that pair-based adaptation performance begins to approach the “Oracle” result trained on 338 real examples.

Finally, we note that, while our discussion of our model here considers a pose estimation task, the combination of loss functions we present here is generic and can be applied to a variety of tasks including classification and detection, so long as paired source-target examples are present.

5 EVALUATION

We demonstrate the effectiveness of our approach on two synthetic-real domain shifts. The first is a simple airplane pose estimation task, in which we attempt to estimate the azimuth of airplanes in PASCAL images (Everingham et al., 2010). The second is a robotic pose estimation task using the Willow Garage PR2, in which we attempt to estimate the position of the PR2 gripper in 3D from images taken from the robot’s camera. In both cases, the presence of pose information allows us to render corresponding synthetic views, which we use to augment our training set and enable improved performance over the real-only baseline.

5.1 PASCAL AIRPLANE POSE ESTIMATION

We begin by demonstrating the applicability of our approach on a simple airplane azimuth estimation task. The PASCAL3D+ dataset (Xiang et al., 2014) provides additional 3D annotations for 12 rigid categories in the PASCAL VOC 2012 dataset (Everingham et al., 2010). We focus on the first of these categories, “airplane,” and consider the task of estimating the azimuth of airplanes relative to the camera viewpoint.

However, to simulate an adaptation setting, in which target data is limited, we train using only 17 real images and augment our training data with synthetic renderings of airplanes, similar to Peng

et al. (2014). We use the pose annotations on these 17 training images to render 3D models in the same pose over simple sky backgrounds. An example of one of these pairs is provided in Figure 3. We additionally render 321 additional synthetic images using the poses from 321 real images, but do not include the corresponding real images themselves. The remaining 338 real images (which are not used to generate synthetic renderings) are used for evaluation.

As a simple experiment, we repurpose the standard architecture of Krizhevsky et al. (2012), replacing the final 1000-way output with a simple 2-way output to regress to the sine and cosine of azimuth. We initialize our model using weights learned on the ImageNet dataset (Russakovsky et al., 2015). Both the domain confusion loss (weighted at $\lambda = 0.01$) and the contrastive loss ($m = 100$, weighted at $\nu = 10^{-5}$), when in use, are applied to the 7th layer. When using both losses together, we further halve the weights applied to each, so that $\lambda = 0.005$ and $\nu = 5 \times 10^{-6}$.

We report the percentage of test examples localized within error thresholds of varying sizes in Table 1. The results indicate that incorporating explicit paired examples into the optimization leads to improved performance on this simple pose estimation task. We also find that, although the domain confusion loss and the contrastive loss perform similarly on their own, combining them provides a further performance increase, indicating that the two losses are complementary.

Finally, if we compare adaptation performance to the ‘‘Oracle’’ setting, in which we train on all of the real training data instead of limiting ourselves to 17 examples, we find that adaptation with paired constraints is able to make up over 40% of the difference in performance over the simple non-adaptive baselines.

5.2 ROBOTIC POSE ESTIMATION

We also evaluate our method on a pose estimation task meant to be representative of the sort of visual estimation required for robotic control. Our task requires estimating the location of the robot’s right gripper. Estimating end-effector positions from visual inputs is a common method for correcting for inaccurate forward kinematics and low-quality encoder readings, which can be present even in high-end robotic systems (Pastor et al., 2013). We train a model to regress to the 3D location of three specific points on the robot’s right gripper, thereby capturing its pose.

We collected pose data of the Willow Garage PR2 robot in both simulation, using the Gazebo simulator, and the real world. All real trials use the PR2’s right wide stereo camera, while the simulation trials use the libgazebo_ros_prosilica sensor placed at the right wide stereo camera’s frame. The matched data is generated by ensuring that the simulation ends at the same end-effector positions as the real world PR2. Although this method of alignment is sensitive to the calibration of the robot, we treat it as part of our domain shift and rely on our adaptation method to apply the appropriate correction. We further note that, due to custom force sensors installed on our PR2, its grippers extend an additional 3.5 centimeters beyond the factory grippers, causing further domain mismatch between the synthetic-real imagery. An example synthetic-real image pair can be seen in Figure 1.

In this setting, our training data consists of 5 synthetic-real image pairs, as well as 1000 additional unpaired synthetic images. Evaluation is done on a held-out set of 500 real images.

For this task, we adopt the deep spatial feature point architecture introduced by Levine et al. (2015). Both the domain confusion loss ($\lambda = 0.1$) and contrastive loss ($m = 1$, $\nu = 0.01$) are applied at the third convolutional layer, after the ReLU nonlinearity. As before, when both losses are employed simultaneously, we further halve each of their weights. Results from this experimental setting are presented in Table 2.

Once again, the results indicate that adaptation with paired examples yields improved performance. Interestingly, we find that despite how visually similar the synthetic and real images may appear, incorporating synthetic imagery during training is nontrivial. Simply combining synthetic and real imagery into one large training set negatively impacts performance, due to slight variations in appearance and viewpoint. We see that domain confusion alone does not help either, since domain confusion does not offer a way to learn the specific viewpoint variations between the real and synthetic domains. Nonetheless, by exploiting the presence of pairs, our method is able to account for these differences, performing better than all other baselines.

Method	Average distance (cm)
Synthetic only	26.37
Real only	4.32
Synthetic and real	6.15
Domain confusion (Tzeng et al., 2015)	6.88
Contrastive loss	4.82
Generalized domain alignment	3.99
Oracle	0.94

Table 2: Evaluation results on PR2 gripper pose estimation when limiting ourselves to only 5 real examples. Once again, each real example is paired with a corresponding synthetic image in the same pose, and an additional 1000 unpaired synthetic images are also provided as training data. The model is trained to output three 3D points that define the pose of the gripper, and we report the average distance from the ground truth points in centimeters. We find that the real only baseline is surprisingly hard to beat and incorporating additional synthetic data is non-trivial. Nonetheless, through combining both a domain confusion loss and a pair alignment loss, we are able to improve performance by 10% (relative).

6 CONCLUSION

In this paper, we present a novel model for domain adaptation that is able to exploit the presence paired source-target examples. Our model extends existing adaptation architectures by applying a well-established contrastive function in an adaptation setting for the first time. Because of its generality, our method is applicable to a wide variety of deep adaptation architectures and tasks. We experimentally validate the importance of using image pairs and show that they are integral to achieving strong adaptation performance.

We address domain adaptation for visual inputs in the context of robotic state estimation. The tasks used in our robotic evaluation involve estimating information that is highly relevant for robotic control (Pastor et al., 2013), as well as for pretraining visuomotor control policies (Levine et al., 2015). While we show successful transfer of simulated data for learning real-world visual tasks, training full control policies in simulation will also require tackling the question of physical adaptation, to account for the mismatch between simulated and real-world physics. Addressing this question in future work would pave the way for large-scale training of robotic control policies in simulation.

REFERENCES

- Aytar, Y. and Zisserman, A. Tabula rasa: Model transfer for object category detection. In *IEEE International Conference on Computer Vision*, 2011.
- Bromley, Jane, Guyon, Isabelle, LeCun, Yann, Säckinger, Eduard, and Shah, Roopak. Signature verification using a “siamese” time delay neural network. In Cowan, J.D., Tesauero, G., and Alspector, J. (eds.), *Advances in Neural Information Processing Systems 6*, pp. 737–744. Morgan-Kaufmann, 1994.
- Chopra, Sumit, Hadsell, Raia, and LeCun, Yann. Learning a similarity metric discriminatively, with application to face verification. In *Computer Vision and Pattern Recognition, 2005. CVPR 2005. IEEE Computer Society Conference on*, volume 1, pp. 539–546. IEEE, 2005.
- Duan, L., Xu, D., and Tsang, Ivor W. Learning with augmented features for heterogeneous domain adaptation. In *Proc. ICML*, 2012.
- Everingham, M., Van Gool, L., Williams, C. K. I., Winn, J., and Zisserman, A. The pascal visual object classes (voc) challenge. *International Journal of Computer Vision*, 88(2):303–338, June 2010.
- Finn, C., Tan, X., Duan, Y., Darrell, T., Levine, S., and Abbeel, P. Learning visual feature spaces for robotic manipulation with deep spatial autoencoders. *arXiv preprint arXiv:1509.06113*, 2015.

- Ganin, Yaroslav and Lempitsky, Victor. Unsupervised domain adaptation by backpropagation. In *International Conference in Machine Learning (ICML)*, 2015.
- Gong, B., Shi, Y., Sha, F., and Grauman, K. Geodesic flow kernel for unsupervised domain adaptation. In *Proc. CVPR*, 2012.
- Gopalan, R., Li, R., and Chellappa, R. Domain adaptation for object recognition: An unsupervised approach. In *Proc. ICCV*, 2011.
- Hadsell, Raia, Chopra, Sumit, and LeCun, Yann. Dimensionality reduction by learning an invariant mapping. In *Proc. Computer Vision and Pattern Recognition Conference (CVPR'06)*. IEEE Press, 2006.
- Hoffman, Judy, Rodner, Erik, Donahue, Jeff, Saenko, Kate, and Darrell, Trevor. Efficient learning of domain-invariant image representations. In *International Conference on Learning Representations*, 2013.
- Krizhevsky, A., Sutskever, I., and Hinton, G. E. ImageNet classification with deep convolutional neural networks. In *Proc. NIPS*, 2012.
- Kulis, B., Saenko, K., and Darrell, T. What you saw is not what you get: Domain adaptation using asymmetric kernel transforms. In *Proc. CVPR*, 2011.
- Levine, Sergey, Finn, Chelsea, Darrell, Trevor, and Abbeel, Pieter. End-to-end training of deep visuomotor policies. *CoRR*, abs/1504.00702, 2015.
- Lillicrap, T. P., Hunt, J. J., Pritzel, A., Heess, N., Erez, T., Tassa, Y., Silver, D., and Wierstra, D. Continuous control with deep reinforcement learning. *arXiv preprint arXiv:1509.02971*, 2015.
- Long, Mingsheng, Cao, Yue, Wang, Jianmin, and Jordan, Michael I. Learning transferable features with deep adaptation networks. In *International Conference in Machine Learning (ICML)*, 2015.
- Mansour, Yishay, Mohri, Mehryar, and Rostamizadeh, Afshin. Domain adaptation: Learning bounds and algorithms. In *COLT*, 2009.
- Mnih, V., Kavukcuoglu, K., Silver, D., Graves, A., Antonoglou, I., Wierstra, D., and Riedmiller, M. Playing Atari with deep reinforcement learning. *NIPS '13 Workshop on Deep Learning*, 2013.
- Pastor, P., Hoffmann, H., Asfour, T., and Schaal, S. Learning and generalization of motor skills by learning from demonstration. In *International Conference on Robotics and Automation (ICRA)*, 2009.
- Pastor, P., Kalakrishnan, M., Binney, J., Kelly, J., Righetti, L., Sukhatme, G., and Schaal, S. Learning task error models for manipulation. In *IEEE International Conference on Robotics and Automation*, 2013.
- Peng, Xingchao, Sun, Baochen, Ali, Karim, and Saenko, Kate. Exploring invariances in deep convolutional neural networks using synthetic images. *CoRR*, abs/1412.7122, 2014. URL <http://arxiv.org/abs/1412.7122>.
- Peng, Xingchao, Sun, Baochen, Ali, Karim, and Saenko, Kate. Learning deep object detectors from 3d models. In *The IEEE International Conference on Computer Vision (ICCV)*, December 2015.
- Pinto, L. and Gupta, A. Supersizing self-supervision: Learning to grasp from 50k tries and 700 robot hours. *arXiv preprint arXiv:1509.06825*, 2015.
- Pomerleau, D. ALVINN: an autonomous land vehicle in a neural network. In *Advances in Neural Information Processing Systems (NIPS)*, 1989.
- Riedmiller, M., Lange, S., and Voigtlaender, A. Autonomous reinforcement learning on raw visual input data in a real world application. In *International Joint Conference on Neural Networks*, 2012.

- Russakovsky, Olga, Deng, Jia, Su, Hao, Krause, Jonathan, Satheesh, Sanjeev, Ma, Sean, Huang, Zhiheng, Karpathy, Andrej, Khosla, Aditya, Bernstein, Michael, Berg, Alexander C., and Fei-Fei, Li. ImageNet Large Scale Visual Recognition Challenge. *International Journal of Computer Vision (IJCV)*, 115(3):211–252, 2015. doi: 10.1007/s11263-015-0816-y.
- Saenko, K., Kulis, B., Fritz, M., and Darrell, T. Adapting visual category models to new domains. In *Proc. ECCV*, 2010.
- Schulman, J., Levine, S., Moritz, P., Jordan, M., and Abbeel, P. Trust region policy optimization. In *International Conference on Machine Learning (ICML)*, 2015.
- Shakhnarovich, Gregory, Viola, Paul, and Darrell, Trevor. Fast pose estimation with parameter-sensitive hashing. In *Computer Vision, 2003. Proceedings. Ninth IEEE International Conference on*, pp. 750–757. IEEE, 2003.
- Su, Hao, Qi, Charles R., Li, Yangyan, and Guibas, Leonidas J. Render for cnn: Viewpoint estimation in images using cnns trained with rendered 3d model views. In *The IEEE International Conference on Computer Vision (ICCV)*, December 2015.
- Sun, Baochen and Saenko, Kate. From virtual to reality: Fast adaptation of virtual object detectors to real domains. In *British Machine Vision Conference (BMVC)*, 2014.
- Taylor, Graham W., Fergus, Rob, Williams, George, Spiro, Ian, and Bregler, Christoph. Pose-sensitive embedding by nonlinear nca regression. In Lafferty, J.D., Williams, C.K.I., Shawe-Taylor, J., Zemel, R.S., and Culotta, A. (eds.), *Advances in Neural Information Processing Systems 23*, pp. 2280–2288. Curran Associates, Inc., 2010.
- Tompson, Jonathan J., Jain, Arjun, Lecun, Yann, and Bregler, Christoph. Joint training of a convolutional network and a graphical model for human pose estimation. In Ghahramani, Z., Welling, M., Cortes, C., Lawrence, N.d., and Weinberger, K.q. (eds.), *Advances in Neural Information Processing Systems 27*, pp. 1799–1807. Curran Associates, Inc., 2014.
- Toshev, Alexander and Szegedy, Christian. Deeppose: Human pose estimation via deep neural networks. *CoRR*, abs/1312.4659, 2013.
- Tzeng, Eric, Hoffman, Judy, Zhang, Ning, Saenko, Kate, and Darrell, Trevor. Deep domain confusion: Maximizing for domain invariance. *CoRR*, abs/1412.3474, 2014.
- Tzeng, Eric, Hoffman, Judy, Darrell, Trevor, and Saenko, Kate. Simultaneous deep transfer across domains and tasks. In *International Conference in Computer Vision (ICCV)*, 2015.
- Urtasun, R. and Darrell, T. Sparse probabilistic regression for activity-independent human pose inference. In *Computer Vision and Pattern Recognition, 2008. CVPR 2008. IEEE Conference on*, pp. 1–8, June 2008. doi: 10.1109/CVPR.2008.4587360.
- Watter, M., Springenberg, J., Boedecker, J., and Riedmiller, M. Embed to control: a locally linear latent dynamics model for control from raw images. In *Advances in Neural Information Processing Systems (NIPS)*, 2015.
- Xiang, Yu, Mottaghi, Roozbeh, and Savarese, Silvio. Beyond pascal: A benchmark for 3d object detection in the wild. In *IEEE Winter Conference on Applications of Computer Vision (WACV)*, 2014.
- Yang, J., Yan, R., and Hauptmann, A. G. Cross-domain video concept detection using adaptive svms. *ACM Multimedia*, 2007.
- Zhang, F., Leitner, J., Milford, M., Upcroft, B., and Corke, P. Towards Vision-Based Deep Reinforcement Learning for Robotic Motion Control. *ArXiv e-prints*, November 2015.